CHEMISTRY
A EUROPEAN JOURNAL

FULL PAPER

DOI: 10.1002/chem.201201906

Hydrogen-Bonded Complexes between 4-Alkoxystilbazoles and Fluorophenols: Solid-State Structures and Liquid Crystallinity

Joanna P.-W. Wong, Adrian C. Whitwood, and Duncan W. Bruce*[a]

Abstract: 48 new hydrogen-bonded complexes have been prepared by combining 16 fluorophenols of general formula $C_6F_nH_{5-n}OH$ with three different alkoxystilbazoles (butyloxy-, octyloxy- and dodecyloxy-). Single-crystal X-ray structures were obtained for 10 of the 16 complexes of octyloxystilbazole from which it was found that most of the structures could be collected into one of two groups according to both the motif shown by the complex and by the solid-state packing. Because all but one crystallised in the $P\bar{1}$ space group, meaningful comparisons could be drawn and it was observed that six structures were extremely close in nature so that significant molecular overlap was found. On this basis, doubt is cast on the significance of some of the weaker intermolecular contacts found in the solid state. 40 of the new complexes showed liquid-crystal properties and it was found that although complexes of butyloxystilbazole were all nematic, almost all of those with dodecyloxystilbazole showed a smectic A (SmA) phase. Complexes of octyloxystilbazole showed a mixture of both. Structure/property correlations showed that clearing points were independent of the pK_a of the phenol. The most stable mesophases were found when the fluorophenol contained a fluorine at the 2-position, which was interpreted in terms of the formation of an intramolecular H···F hydrogen bond to give a six-membered ring linking the two components into a stable, coplanar conformation. The least stable mesophases were found when no such ring formation was possible and the phenol was relatively free to move.

Keywords: fluorophenols · hydrogen bonding · liquid crystals · stilbazoles · X-ray diffraction

Introduction

Liquid crystals are the original supramolecular materials because their mesophases are stabilised by non-covalent, intermolecular interactions, namely anisotropic dispersion forces that arise from the anisometric nature of the materials giving rise to the phases. However, in addition, specific intermolecular interactions may be employed to modify liquid-crystal behaviour or even to induce it through the interaction of non-mesomorphic components.[1] One such interaction that has been described in recent years is halogen bonding,[2] which is an attractive, electrostatic interaction between a halogen atom (normally iodine) that is electron poor and a Lewis base (most often nitrogen). Thus, through the supramolecular chemistry pioneered in Milan,[3] halogen bonding has become a more widely used interaction in the formation of what can be quite complex supramolecular species.

Halogen bonding may be regarded as formally analogous to the better-known hydrogen bonding, and it was through this analogy that our interest in the subject grew. Thus, Kato and Fréchet and their co-workers[4] did a great deal to reinvigorate work into hydrogen bonding in liquid crystals using a conceptually simple and elegant approach (Figure 1). With

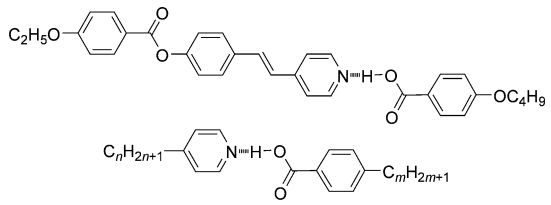

Figure 1. Examples of hydrogen-bonded mesogens reported by Kato, Fréchet and co-workers.

that inspiration, previous work from this group reported on liquid-crystalline complexes formed from stilbazoles and various phenolic[5] and other[6] species (Figure 2), while others have built elegant structures of higher symmetry using complementary bonding approaches.[7]

However, more recently aware of halogen bonding, we published the first example of a liquid-crystalline material formed using a halogen bond, namely a halogen-bonded complex between an alkoxystilbazole and iodopentafluorobenzene.[8] Other examples followed quickly both from ourselves[9] and others.[10] In wishing to extend this work, we

[a] J. P.-W. Wong, Dr. A. C. Whitwood, Prof.Dr. D. W. Bruce
Department of Chemistry
University of York
Heslington
YORK YO10 5DD (UK)
Tel: (+44) 1904-324085
E-mail: duncan.bruce@york.ac.uk

Supporting information for this article is available on the WWW under http://dx.doi.org/10.1002/chem.201201906.

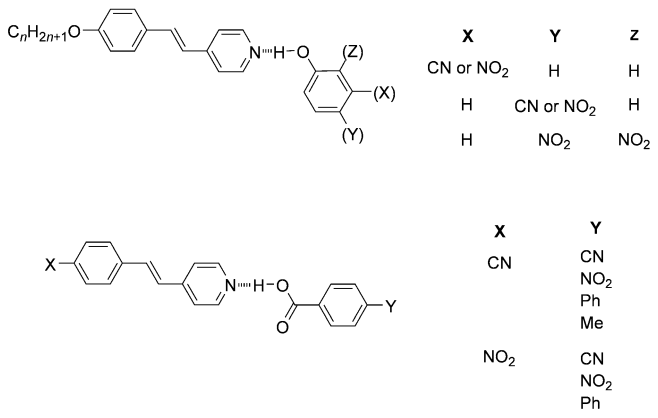

Figure 2. Hydrogen-bonded phenols and other systems prepared previously in this group.

had hoped to prepared and study a range of complexes based on alkoxystilbazoles and various isomers of iodofluorobenzenes, $C_6F_nH_{5-n}I$, but many of these proved resistant to crystallisation and so we undertook a related, structure-only study of co-crystals formed between $C_6F_nH_{5-n}I$ and 4-(*N,N*-dimethylamino)pyridine (DMAP).[11] One of the things that emerged from that study was a very good correlation between the length of the halogen bond, d(N···I), and the number of fluorine atoms on the ring. This correlation improved further when d(N···I) was plotted against the calculated pK_a values for the related phenol, $C_6F_nH_{5-n}OH$ (Figure 3),[12] for which the pK_a is, of course, a measure of the stability of $C_6F_nH_{5-n}O^-$, which is in turn a proxy for the development of positive electrostatic potential on the iodine atom of $C_6F_nH_{5-n}I$.

Encouraged by these studies, it then became attractive to undertake a systematic study of the structure and liquid-

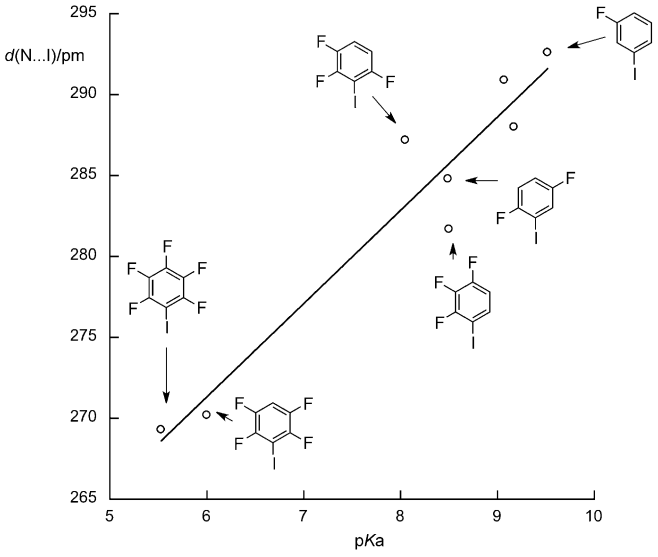

Figure 3. Plot of calculated pK_a of $C_6F_{5-n}H_nOH$ versus d(N···I) for a series of co-crystals of DMAP with $C_6F_{5-n}H_nI$. Adapted from ref. [10] © American Chemical Society 2009.

crystallinity of stilbazole complexes of fluorophenols from which one might learn about the way both hydrogen bond strength and level and pattern of fluorine substitution affected mesomorphism.

In planning the study, a decision was made to use stilbazoles with three different chain lengths, namely C4, C8 and C12, with the rationale that complexes of the shortest homologue ought to be dominated by the formation of the nematic phase, whereas complexes of the longest homologues would be dominated by smectic phases (probably SmA), with the C8 derivatives showing a mixture of both. Insofar as the phenols are concerned, there are 19 isomers of $C_6F_nH_{5-n}OH$ with $n \neq 0$ (see Figure S1 in the Supporting Information) of which 16 were chosen for study leading to 48 new complexes that were prepared and studied for their liquid-crystal properties. In considering an accompanying structural study, a decision was made to look at complexes of octyloxystilbazole and to this end, single-crystal structures were obtained for 10 of the possible 16 complexes, along with 1 complex of a butyloxystilbazole.

Results

The hydrogen-bonded complexes to be studied were prepared by separately dissolving the appropriate stilbazole and fluorophenol in the same solvent and then combining the two solutions with stirring at room temperature for 1.5 hours. Pentane was used as the solvent for complexation for the 4-butoxy-4′-stilbazole and 4-octyloxy-4′-stilbazole homologues, whereas hexane was preferred for the 4-dodecyloxy-4′-stilbazole complexes. The 1:1 composition of the crystalline complexes so obtained was established by elemental analysis and the data are given in Table S1 (in the Supporting Information). Complexes of pentafluorophenol were a pale yellow colour and, as the degree of fluorination decreased, the yellow colour became ever paler so that complexes of the three monofluorophenols were colourless. The colour has its origin in the degree of proton transfer to the stilbazole nitrogen. Thus, previously we showed that although pure stilbazoles had $\lambda_{max} = 320$ nm, the fully protonated stilbazolium cation absorbs at 390 nm,[5a] the significant shift being in large part due to the fact that alkoxystilbazoles are good chromophores for quadratic non-linear optical processes.[13] That the absorption maximum is sensitive to the position of the hydrogen in the N···H–O hydrogen bond is something we used previously to demonstrate proton transfer in the liquid-crystal phase behaviour of alkoxystilbazoles with 2,4-dinitrophenol.[5b]

To study the solid-state behaviour of these complexes, those from octyloxystilbazole were chosen and structures were determined for 10 of the 16 complexes prepared. The single crystals were obtained from pentane or hexane at ambient temperature or 4 °C, and selected crystallographic data are collected in Table 1. A majority of the complexes crystallised as bunches of needles growing from a single nucleation point, whereas some grew as plates and others blocks.

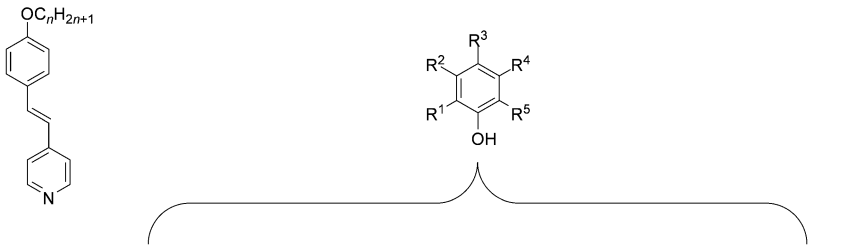

Scheme 1. The three different stilbazoles used in combination with different fluorinated phenols; all R^x substituents are hydrogen where not indicated as fluorine.

The complexes formed are numbered according to the representations shown in Scheme 1.

All short contacts were defined as being less than the sum of the van der Waals radii minus 0.1 Å ([ΣvdW−0.1] Å). It is instructive to note that all but one complex (**2-4c**) crystallised in the space group $P\bar{1}$ and so comparisons between them are meaningful. The discussion of the complexes is grouped so that those with similar arrangements in the solid state are treated together. In addition, crystals were obtained of complex **1-6e** for which the structure is reported although not discussed in any detail.

Description of the crystal structures

*Complex **1-6e***: The complex crystallised without disorder. The two stilbazole rings were close to co-planar (angle between planes = 5.06°) and the fluorophenol ring was bound to the pyridyl nitrogen through a hydrogen bond of length 1.708 Å, which was reasonably close to linear at 171.31°. The fluorophenyl ring made an angle of 68.61° to the pyridyl ring of the stilbazole (Figure 4). The packing of this complex is closest to that of **2-5a**, **2-5d**, **2-5f**, **2-4a** and **2-4b** described below.

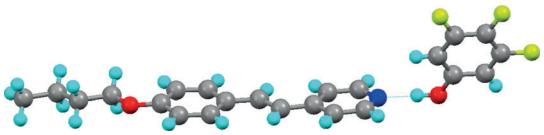

Figure 4. Molecular structure of complex **1-6e**.

*Complexes **2-8**, **2-7** and **2-6b***: Complex **2-8** is disordered and so both of the aromatic rings and the double bond of the stilbazole exhibited disorder and were modelled in two positions, the relative occupancy of which refined to 0.77:0.23. For the minor component the aromatic rings were constrained to be regular hexagons with a bond length of 1.39 Å. The atomic displacement parameters (ADP) of corresponding pairs of disordered atoms for example, C7a and C7b, were constrained to be equal. All subsequent treatment and analysis of **2-8** uses a modified cif file that contains the stilbazole in its major site occupancy.

Thus, complexes **2-8**, **2-7** and **2-6b** were found to be nearly planar (Figure 5) and the angles that the planes of the pyridine rings make with the fluorophenol rings were 7.82°, 5.84° and 1.85°, respectively. The N···H–O bonds (Figure 6) were found at an angle of 170.96°, 165.11° and 158.01°, respectively, and

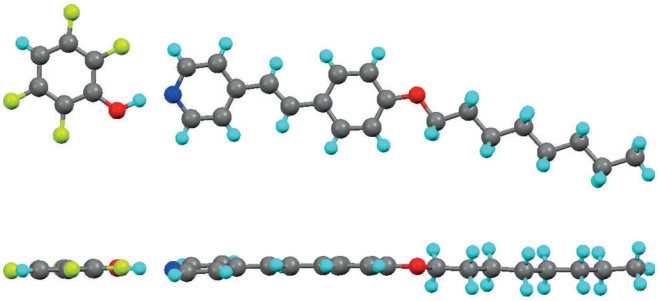

Figure 5. Top and side view of the molecular structure of complex **2-7**.

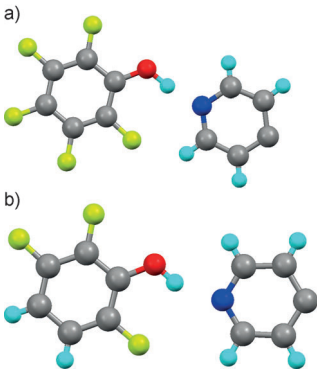

Figure 6. The interaction between the phenolic hydrogen and the pyridine in a) **2-8** and b) **2-6b**.

the corresponding hydrogen bond lengths, $d_{N\cdots H}$ were 1.553, 1.507 and 1.729 Å. For **2-8** and **2-7**, the planar structure led to (or perhaps resulted from) a second interaction between an *ortho* hydrogen on the pyridine ring and a fluorine *ortho* to the hydroxyl function on the phenol; the distances were 2.234 Å (**2-8**) and 2.360 Å (**2-7**). In **2-6b**, the same distance was 3.081 Å, the increased distance resulting from the bending back of the phenol, which was reflected in the smaller N···H–O bond angle.

Two molecules of the complex then dimerise with the phenols aligned back-to-back. In complex **2-8**, the back-to-

Table 1. Selected crystallographic properties of the hydrogen-bonded complexes.

	2-8	**2-7**	**2-6b**	**2-6e**	**2-5a**	**2-5d**
CCDC[a]	884513	884522	884517	884515	884516	884518
F-substitution	2,3,4,5,6	2,3,5,6-	2,3,6-	3,4,5-	2,3-	2,6-
fluorophenol pK_a	5.50	5.91	6.49	8.60	8.65	7.07
d(N···H) [Å]	1.553	1.507	1.729	1.685	1.667	1.580
$\theta_{N\cdots H\text{-}O}$ [°]	170.96	165.11	158.01	177.08	173.20	167.99
space group	$P\bar{1}$	$P\bar{1}$	$P\bar{1}$	$P\bar{1}$	$P\bar{1}$	$P\bar{1}$
crystal system	triclinic	triclinic	triclinic	triclinic	triclinic	triclinic
unit cell dimensions [Å]	a=5.6909(10)	a=5.6936(15)	a=6.1720(3)	a=10.4066(6)	a=7.7812(9)	a=7.7808(10)
	b=12.661(2)	b=12.539(3)	b=11.3711(5)	b=14.3652(8)	b=9.7838(11)	b=9.6495(11)
	c=16.824(3)	c=16.714(4)	c=16.6214(7)	c=15.9121(8)	c=15.2278(17)	c=15.3919(19)
unit cell angles [°]	α=99.906(4)	α=99.854(5)	α=89.5710(10)	α=87.7860(10)	α=87.505(2)	α=92.913(3)
	β=95.535(4)	β=95.866(5)	β=89.5410(10)	β=85.4180(10)	β=89.314(2)	β=90.091(3)
	γ=92.599(4)	γ=92.065(5)	γ=81.6710(10)	γ=87.0740(10)	γ=88.837(2)	γ=90.415(3)
volume [Å^3]	1186.2(4)	1167.7(5)	1154.17(9)	2366.6(2)	1157.9(2)	1154.1(2)
Z	2	2	2	4	2	2
final R indices [I>2σI]	R_1=0.0370,	R_1=0.0482,	R_1=0.0422,	R_1=0.0434,	R_1=0.0448,	R_1=0.0439,
	wR_2=0.0906	wR_2=0.1047	wR_2=0.1194	wR_2=0.1110	wR_2=0.1154	wR_2=0.0953
R indices (all data)	R_1=0.0622,	R_1=0.1066,	R_1=0.0473,	R_1=0.0648,	R_1=0.0546,	R_1=0.0632,
	wR_2=0.1034	wR_2=0.1249	wR_2=0.1256	wR_2=0.1245	wR_2=0.1235	wR_2=0.1067
largest diff. peak and hole [e Å^{-3}]	0.205 and −0.177	0.209 and −0.257	0.484 and −0.255	0.315 and −0.202	0.314 and −0.239	0.181 and −0.187

	2–5f	**2–4a**	**2–4b**	**2–4c**	**1–6e**
CCDC[a]	884512	884519	884520	884514	884521
F-substitution	3,5-	2-	3-	4-	3,4,5-(C4 stilb)
fluorophenol pK_a	8.66	8.73	9.29	9.89	8.60
d(N···H)/Å	1.707	1.714	1.716	1.828	1.708
$\theta_{N\cdots H\text{-}O}$ [°]	176.82	175.86	175.53	169.59	171.31
space group	$P\bar{1}$	$P\bar{1}$	$P\bar{1}$	$P\bar{1}$	$P\bar{1}$
crystal system	triclinic	triclinic	triclinic	orthorhombic	triclinic
unit cell dimensions [Å]	a=7.7371(4)	a=7.8382(11)	a=7.6690(9)	a=14.4911(7)	a=9.4570(11)
	b=9.7508(5)	b=9.5985(13)	b=9.8547(11)	b=6.1494(3)	b=9.6167(12)
	c=15.436(8)	c=15.231(2)	c=15.2857(17)	c=51.527(3)	c=12.9396(16)
unit cell angles [°]	α=92.6130(10)	α=88.188(3)	α=86.725(2)	α=90	α=76.006(2)
	β=90.0900(10)	β=89.391(3)	β=89.923(2)	β=90	β=77.024(2)
	γ=91.7080(10)	γ=87.520(3)	γ=88.706(2)	γ=90	γ=60.548(2)
volume [Å^3]	1162.83(10)	1144.2(3)	1153.0(2)	4591.7(4)	986.5(2)
Z	2	2	2	8	2
final R indices	R_1=0.0442,	R_1=0.0422,	R_1=0.0435,	R_1=0.0497,	R_1=0.0489,
[I>2σI]	wR_2=0.1141	wR_2=0.1077	wR_2=0.1192	wR_2=0.1145	wR_2=0.1317
R indices (all data)	R_1=0.0537,	R_1=0.0590,	R_1=0.0614,	R_1=0.0615,	R_1=0.0574,
	wR_2=0.1218	wR_2=0.1178	wR_2=0.1338	wR_2=0.1223	wR_2=0.1415
largest diff. peak and hole [e Å^{-3}]	0.283 and −0.215	0.331 and −0.233	0.305 and −0.221	0.305 and −0.209	0.589 and −0.258

[a] CCDC numbers given contain the supplementary crystallographic data for this paper. These data can be obtained free of charge from The Cambridge Crystallographic Data Centre via www.ccdc.cam.ac.uk/data_request/cif.

back dimers are offset and are connected by two F···F contacts at 2.719 Å (Figure 7a), with the distance between the planes of the two parallel pentafluorophenol rings being 0.22 Å. The fluorophenols then propagate perpendicular to the dimer through F···F contacts of 2.792 Å between fluorine atoms *para* to the phenol oxygen with the two parallel rings separated by 2.707 Å (Figure 7b). The offset nature of the stacking F···F contacts may suggest that they arise through crystal packing effects and that perhaps they are not strongly structure directing.

The stilbazole/pentafluorophenol unit is then dimeric in the solid state and these dimers propagate laterally into sheets, perhaps through the presence of intermolecular H···F contacts of 2.46 Å between a fluorine *ortho* to the phenolic oxygen and a hydrogen *meta* to the pyridine nitrogen (Figure 8a). This contact is present in **2-7** and **2-6b**, where it is slightly shorter (see below). Formally, there is also another F···F (2.78 Å) and even an H···H (2.27 Å) contact showing up, but it is contended that these are probably not structure directing. In **2-7** (Figure 8b), the dimers are connected by two contacts between F3 and H4 (2.396 Å), whereas there are no such hydrogen–fluorine contacts in **2-6b** (Figure 8c). As in **2-8**, the two fluorophenol rings in **2-7** and **2-6b** are coparallel, their planes being separated by 0.547 and 0.272 Å, respectively.

These dimers then drive the structure packing by arranging side-by-side in a slipped fashion, so that two fluorophenol rings lie next to the two aromatic rings in the stilbazole

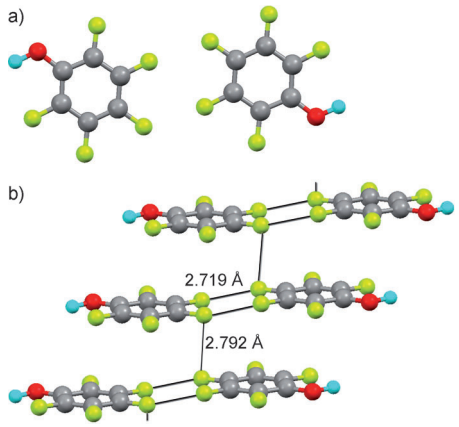

Figure 7. Side-to-side (a) and vertical (b) arrangement of the pentafluorophenol units in **2-8**, the latter being tilted in view and showing F···F contacts.

of a neighbouring dimer. This packing forms a flat, one-dimensional ribbon-like layer, which may be supported by various short contacts. For example, in **2-7** there are intermolecular H···F contacts at 2.408 and 2.454 Å (Figure 8b), whereas in **2-6b** intermolecular H···F contacts are found at 2.354 and 2.611 Å (Figure 8c).

The stacking of the fluorophenol units in **2-8** is reflected in the packing orthogonal to the sheets shown in Figure 8a, and so a kind of segregated structure propagates as shown in Figure 9a. The situation for **2-7** appears very similar when viewed from the side (Figure 9b), but the difference is that there are no short, intermolecular contacts in the stacking direction and in fact the offset of the rings is different in **2-8** and **2-7** when viewed from above (Figure S2 in the Supporting Information). In **2-6b**, there is no apparent segregation in the stacking direction (Figure 9c).

Complex 2-6e: Although still in the $P\bar{1}$ space group, the most significant feature of **2-6e** is that the fluorophenol ring is no longer co-planar with the stilbazole. The structure is most easily described at the local level by considering the existence of a dimeric unit that consists of two face-to-face fluorophenols arranged so that the two O–H vectors are for-

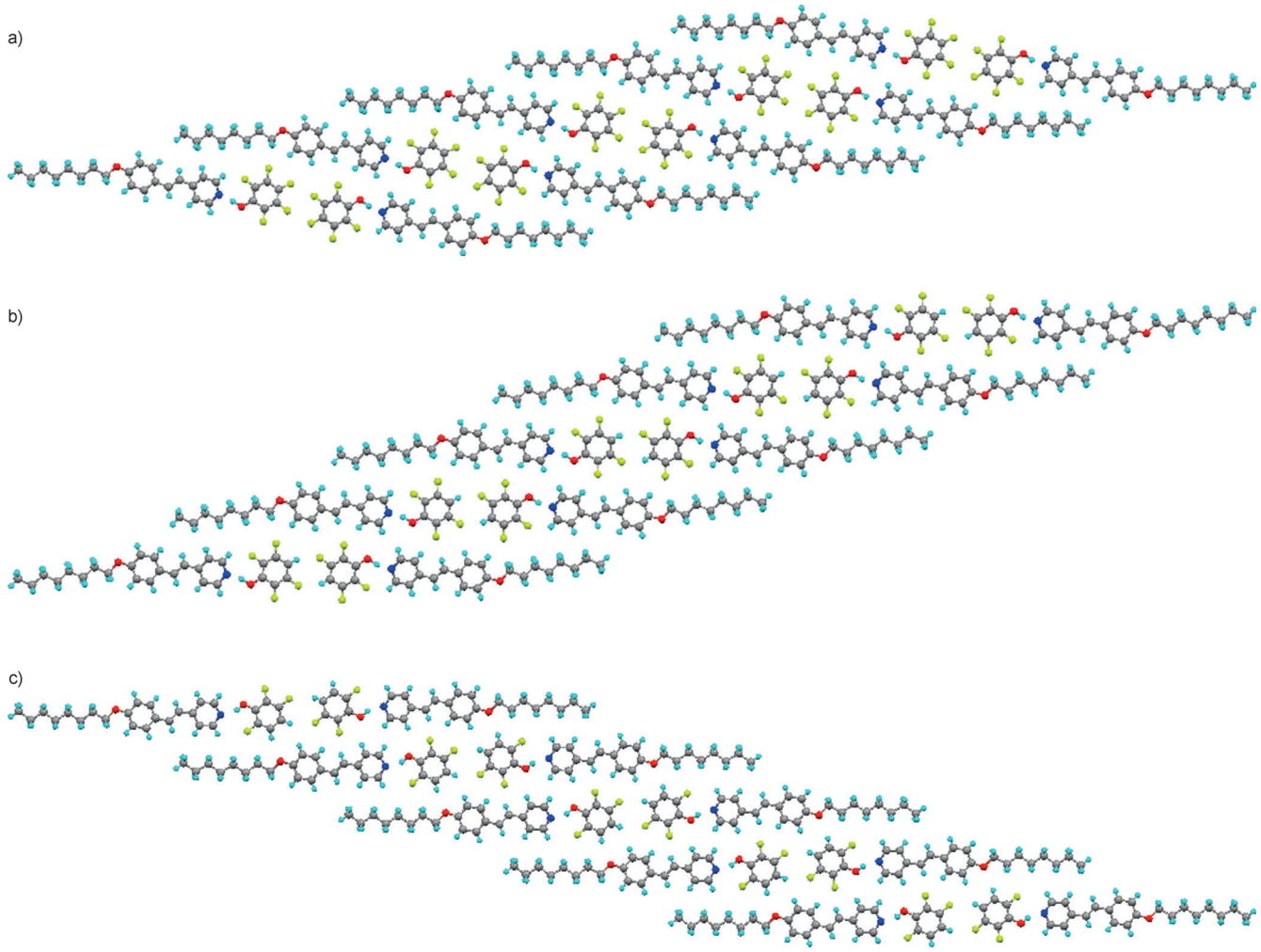

Figure 8. Sheet-like arrangement in the crystal packing of a) complex **2-8**, b) complex **2-7** and c) complex **2-6b**.

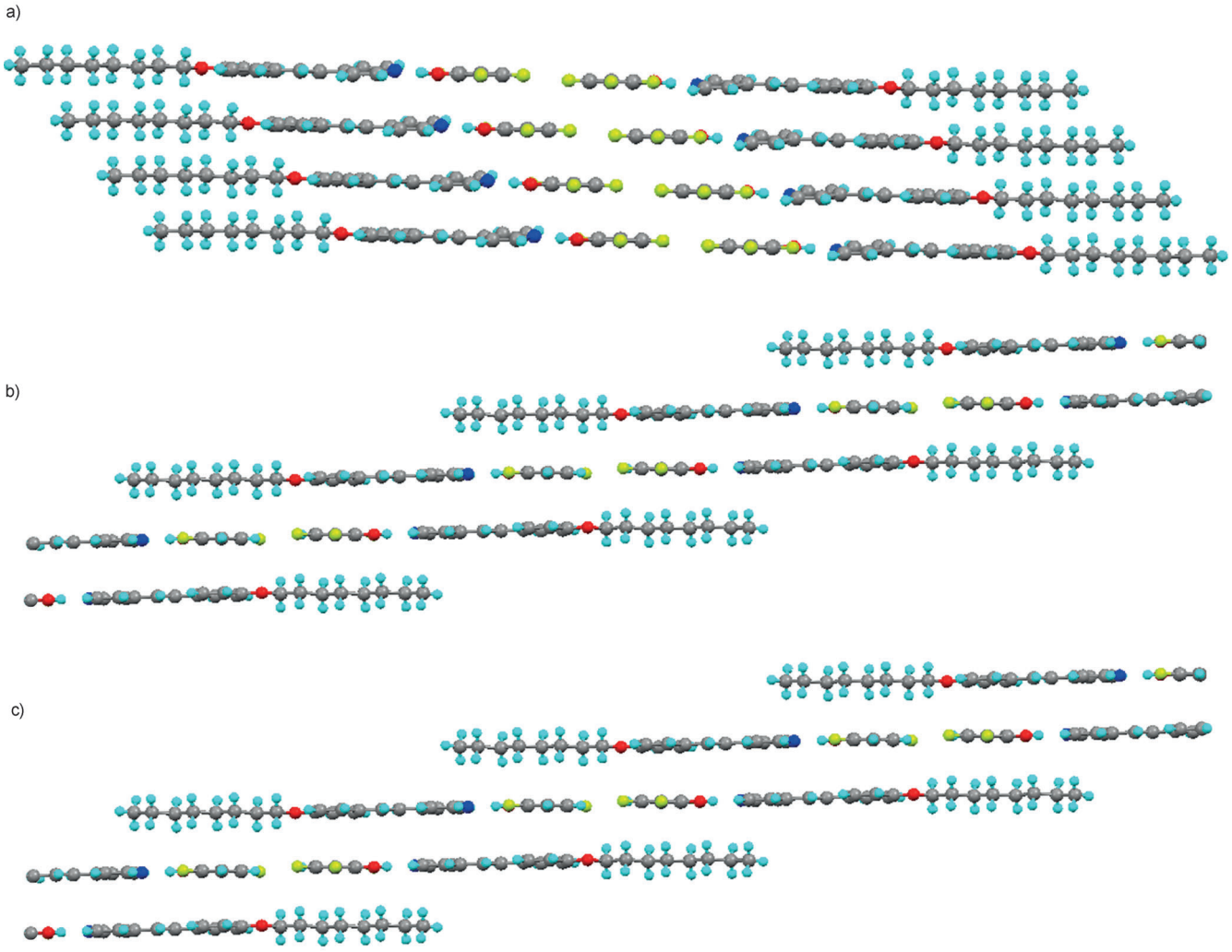

Figure 9. Stacking of complexes a) **2-8**, b) **2-7** and c) **2-6b**.

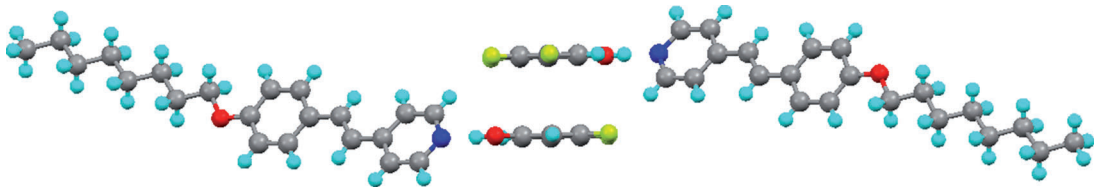

Figure 10. The molecular structure of complex **2-6e** showing the general dimeric arrangement and the orthogonality of the stilbazole and phenol.

mally anti to one another through an inversion centre and are then hydrogen bonded to a stilbazole (Figure 10). Two different types of these dimers make up the crystal structure of **2-6e**, termed dimer A and dimer B. Dimer A forms through the stacking of two fluorophenol rings, which interact through a π–π interaction with an interplane separation of 3.248 Å.

Viewed from above, the fluorophenols are stacked with a displacement of a C−C bond length (Figure 11a). Dimer B differs in that the two fluorophenol planes are separated by a greater distance, 3.413 Å, which suggests a weaker π–π interaction. Such a conclusion is supported by viewing the dimer from above (Figure 11b) where it can be seen that the degree of face-to-face overlap is very much less. In dimer A, the N···H hydrogen bond is 1.685 Å with an N···H–O angle of 177.09°, whereas in dimer B, the hydrogen bond is longer at 1.729 Å, although the angle is very similar at 176.98°. In dimer A, the angle between the pyridine ring and the fluorophenol ring planes is 58.37°, whereas in dimer B it is 58.23°.

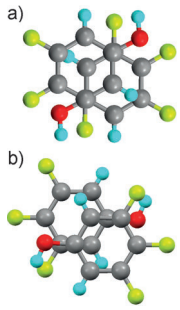

Figure 11. View of the two different dimeric arrangements of phenolic groups in the structure of complex **2-6e** a) dimer A and b) dimer B (see text).

The dimer then lines up side-by-side in a stepped fashion to form a flat "segment" as shown in Figure 12, with all stilbazole rings almost co-planar or flat. Two dimer pairs are linked by two short contacts between O1 and H7, 2.531 Å in length (97.0% of the sum of the vdW radii). Two "segments" then fit together through an interdigitation of the stilbazole alkoxy chains (Figure 12), while still keeping all stilbazole aromatic rings in plane. This extends the layer into an infinite sheet of dimer A or dimer B in the *xy* plane.

*Complexes **2-5a**, **2-5d**, **2-5f**, **2-4a** and **2-4b***: Of these complexes, **2-5a** and **2-4b** were disordered. In the former, the difluorophenyl group was disordered by rotation about the C1–C4 axis, which was modelled in two positions with a refined relative occupancy of 84:16. In the latter, the position of the fluorine was disordered over the two possible *meta* positions, with the relative occupancy being refined to 3:1. In each case, a modified cif file was used to create structures with the disorder removed.

These complexes, which crystallised in the $P\bar{1}$ space group, shared comparable unit cell dimensions (Table 1), dimer structures and crystal packing, although unit cell angles were found as a group of three (**4a**, **4b**, **5a**) and as a group of two (**5d**, **5f**). The fluorophenol rings were twisted between 62.76° and 64.81° out of the plane of the pyridine ring. All of the complexes adopt the same basic structure, which is described in detail for **2-5a**. The only variation of any significance is the way in which the fluorophenol rings pair up in a back-to-back fashion.

Complex **2–5a** crystallised with the fluorophenol ring twisted out of the plane of the pyridine ring by 65.72°, whereas the angle between the aromatic planes of the stilbazole moiety is 16.22°; both such angles are ranked the largest among all the crystal structures obtained (Figure 13a). The hydrogen-bond length is 1.667 Å and the angle at hydrogen is 173.2°. The fluorophenol ring forms a back-to-back dimer with another fluorophenol ring through two F···F contacts of 2.833 Å and the distance between the planes of these two rings in 1.851 Å (Figure 13b).

The structure propagates in the *ac* plane as follows. The pyridine ring of each stilbazole forms a π–π interaction with another stilbazole in an antiparallel fashion with a ring plane separation of 3.262 Å (Figure 14a). As was the case with the two fluorophenol rings in complex **2-6e**, the rings are slipped by one C–C bond length. This stilbazole then hydrogen bonds into one end of a back-to-back difluorophenol dimer, at the other end of which is a second stilbazole above which is a further stilbazole and so the motif continues (Figure 14b).

In complex **2-5d**, the angle between the planes of the pyridine and fluorophenol rings is 64.81°, whereas the two stilbazole aromatic rings made an angle of 13.29°. Within the crystal, there are no short intermolecular contacts that could reasonably be defined as structure directing (recall that the cut-off used is 0.1 Å less than the sum of the van der Waals radii). The dimer motif (Figure 15) of the fluorophenol sees the closest approach of a hydrogen and a fluorine from different rings (2.627 Å), but neither the distance nor the geometry of the relationship suggests that this is very significant. The planes of the two fluorophenol rings are separated by 1.448 Å. The structure propagates in the *ac* plane in the same way as **2-5a**.

Complex **2-5f** has its fluorophenol ring twisted out of the pyridine plane by 62.76° whereas the aromatic rings in the stilbazole subtend an angle of 15.46° between their respective planes. This structure is also lacking in significant intermolecular contacts that might be regarded as structure directing, except for a H···F contact at 2.513 Å between a *meta* hydrogen of a pyridine ring and the fluorine of a neighbouring fluorophenol unit. These propagate to give, in effect, half of the dimer-type organisation seen here, analo-

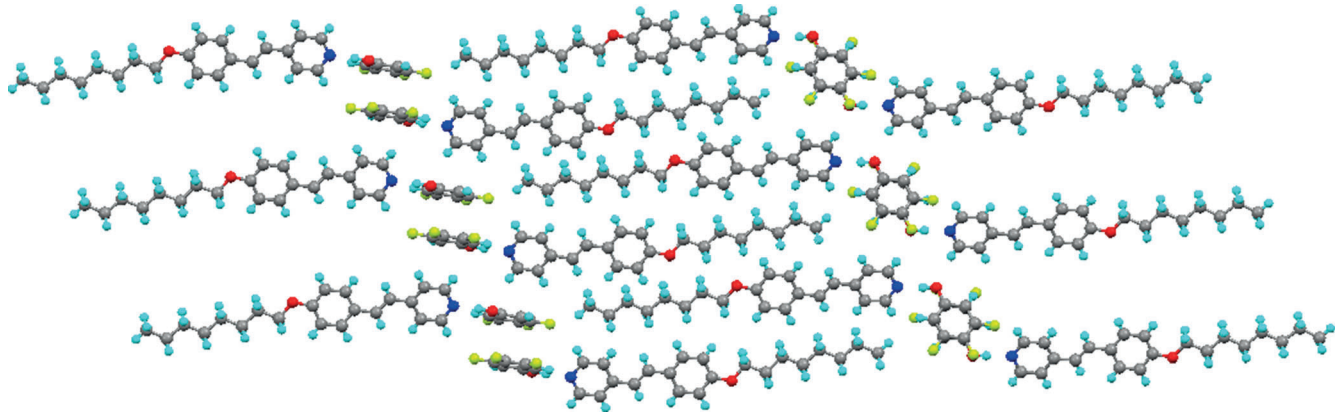

Figure 12. View of the propagation of the complexes in the *ac* plane. Stacks of dimer A are on the left-hand side, whereas those of dimer B are on the right-hand side. The view eclipses the fluorophenol rings on the right.

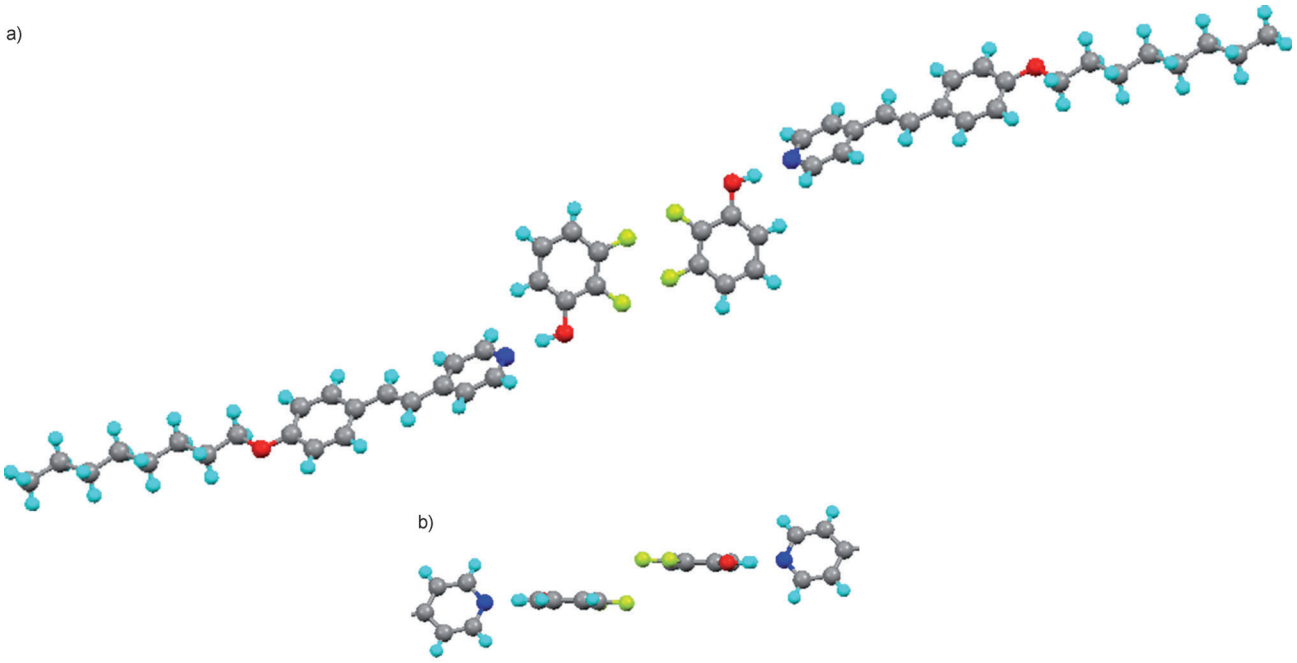

Figure 13. a) Molecular structure of complex **2-5a** and b) a side view showing the back-to-back disposition of the phenolic rings.

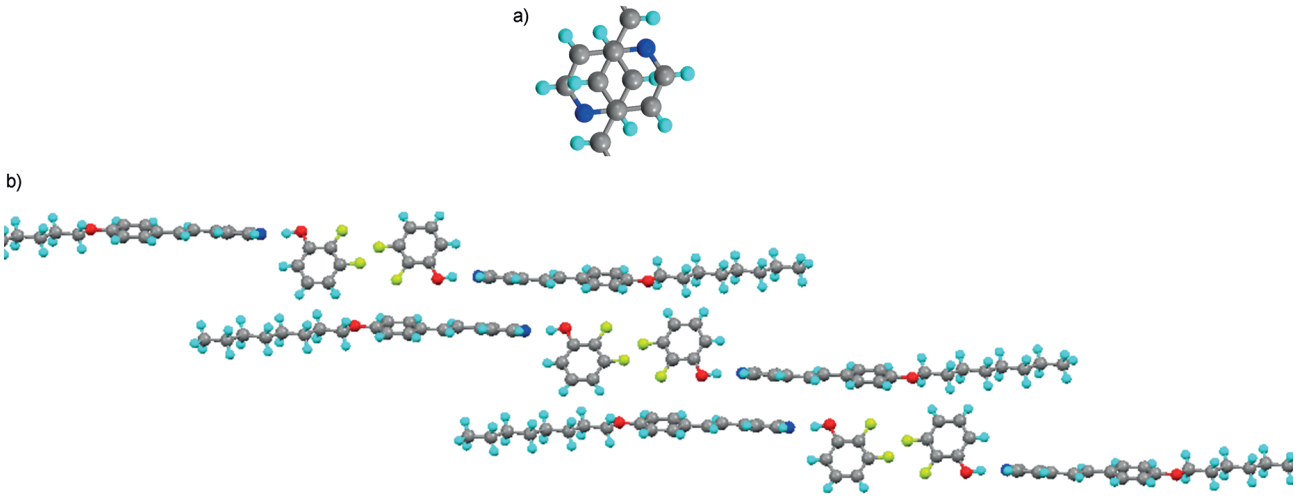

Figure 14. a) Top view of the superposition of the pyridine rings of two antiparallel stilbazole moieties and b) propagation of complex **2-5a** in the *ac* plane.

gous to that in **2-5a** and **2-5d**. The back-to-back dimer is not really supported in any way through the fluorophenol rings because the closest intermolecular separation is an H···F separation of 2.619 Å (Figure 16).

In complex **2-4a**, an N···H–O angle was found that was very nearly linear at 175.86°, and the two stilbazole aromatic rings were almost co-planar making an angle of 14.69° between the two planes. The fluorophenol ring was, however, not co-planar with the stilbazole, being twisted 64.40° out of the plane of the pyridine ring. The primary building block in the crystal structure was the antiparallel, back-to-back dimer (Figure 17) supported by two short intermolecular F···H short contacts (2.549 Å) interacting in a stepped structure identical to those described before.

Finally here, in complex **2-4b** (Figure S3 in the Supporting Information) the organisation is effectively the same as that found for **2-5f**, with an unsupported dimer (H···F distance of 2.614 Å) and a propagating F···H(*meta*) contact of 2.533 Å.

In considering the fact that the five structures above were very closely related, further comparison showed that in four cases of a possible ten, the stilbazole unit from different structures could effectively be overlaid precisely, namely **2-4a** with **2-5f**, and all combinations of **2-4b**, **2-5a** and **2-5d**.[14]

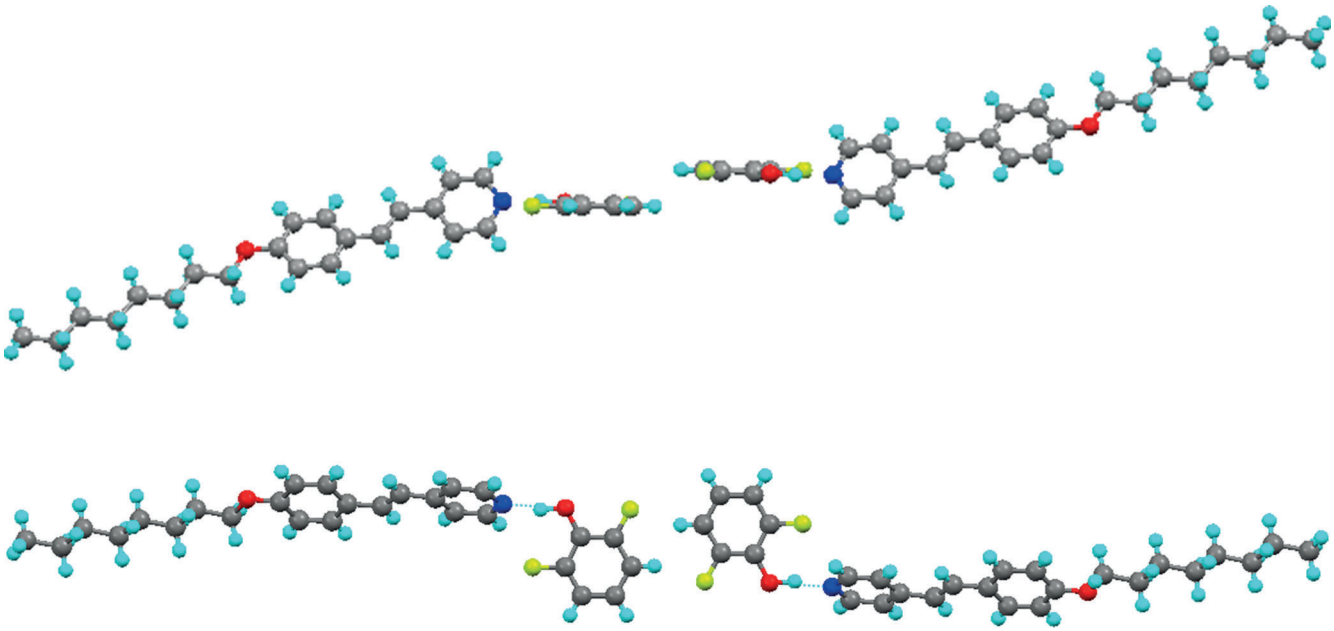

Figure 15. Two orthogonal views of the molecular structure of complex **2-5d**.

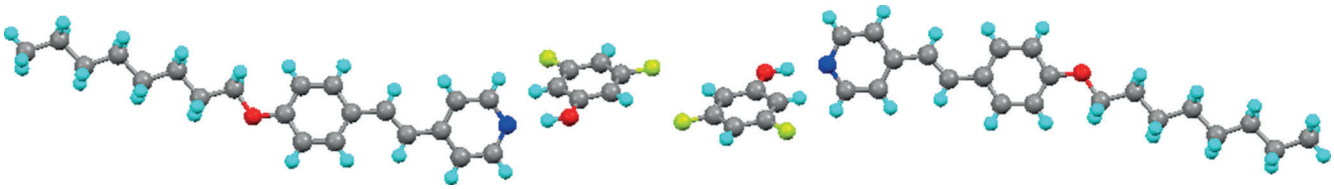

Figure 16. Molecular structure of complex **2-5f**.

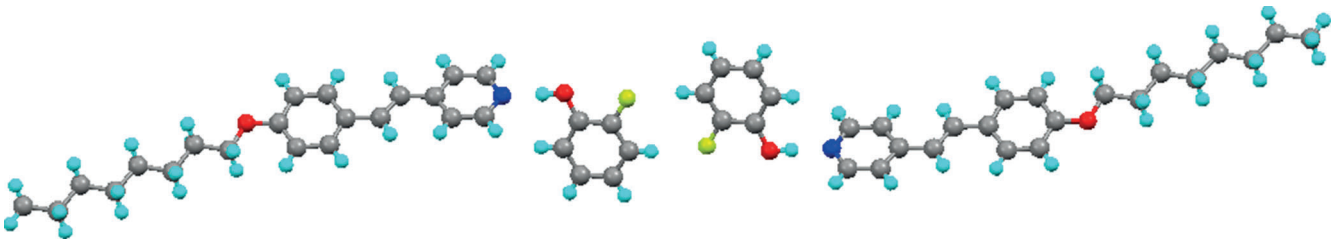

Figure 17. Molecular structure of complex **2-4a**.

In none of these cases did the fluorophenols overlap precisely and some small deviation was seen in the overlap of the terminal alkyl chains. An example is shown as Figure 18, whereas the remaining pairwise combinations are found in Figure S4 (in the Supporting Information).

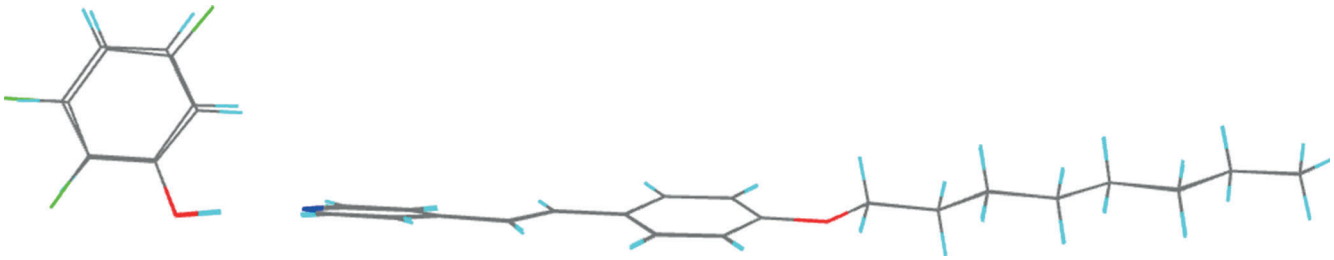

Figure 18. Overlay of complexes **2-4a** and **2-5f**.

That the structures of these complexes are so similar, that they are in the same space group with very similar unit cell dimensions and to some extent angles, and that some may be almost precisely overlaid is a point of note. Indeed, combined with the fact that some structures appear to have short intermolecular contacts, whereas others have few or none, perhaps the question may be posed as to whether such interactions have any great structure-directing effect, or whether they are largely a consequence of the efficient crystallisation of the complexes. These observations do, however, suggest that interpretation of intermolecular contacts requires both care and criticality.

*Complex **2-4c***: Complex **2-4c** was unique among those studied because it crystallised in the *Pbca* space group and had comparatively large unit cell dimensions. The two components of the **2-4c** complex are bound through a hydrogen bond (1.828 Å) with a N···H–O angle of 169.59°. The aromatic rings in the stilbazole are nearly co-planar making an angle of 7.50°, whereas the fluorophenol ring is twisted out of the plane of the pyridine ring by 23.26° (Figure S5 in the Supporting Information). There are no short contacts that could be described as structure directing.

The crystal packing of the **2-4c** complex sees a polar, zig-zag arrangement that propagates in the *bc* plane (Figure 19), whereas in the *a* direction, the next such plane has an opposite net polarisation, consistent with the symmetry of the space group.

Other structural correlations: The other property that it is instructive to correlate is the calculated pK_a of the phenols with the length of the N···H hydrogen bond and also with the N···H–O angle. Correlation with the latter is not convincing (Figure S6a in the Supporting Information), which is perhaps not surprising given that there is relatively little angular preference in hydrogen bonding, but there is a correlation with hydrogen bond length (Figure 20). In this case, data for **2-4c** are removed (because it crystallises in a different space group) as are data for **2–6c** (the unedited plot is found as Figure S6b in the Supporting Information) to give a straight line of correlation 0.973. Given the range of factors affecting packing in the solid state, it is remarkable that such a good correlation is found. It is also noted that in none of the cases is the stilbazole protonated, which is consistent with the pale yellow colour observed for complex **2-8** that contains the most acidic phenol (see above).

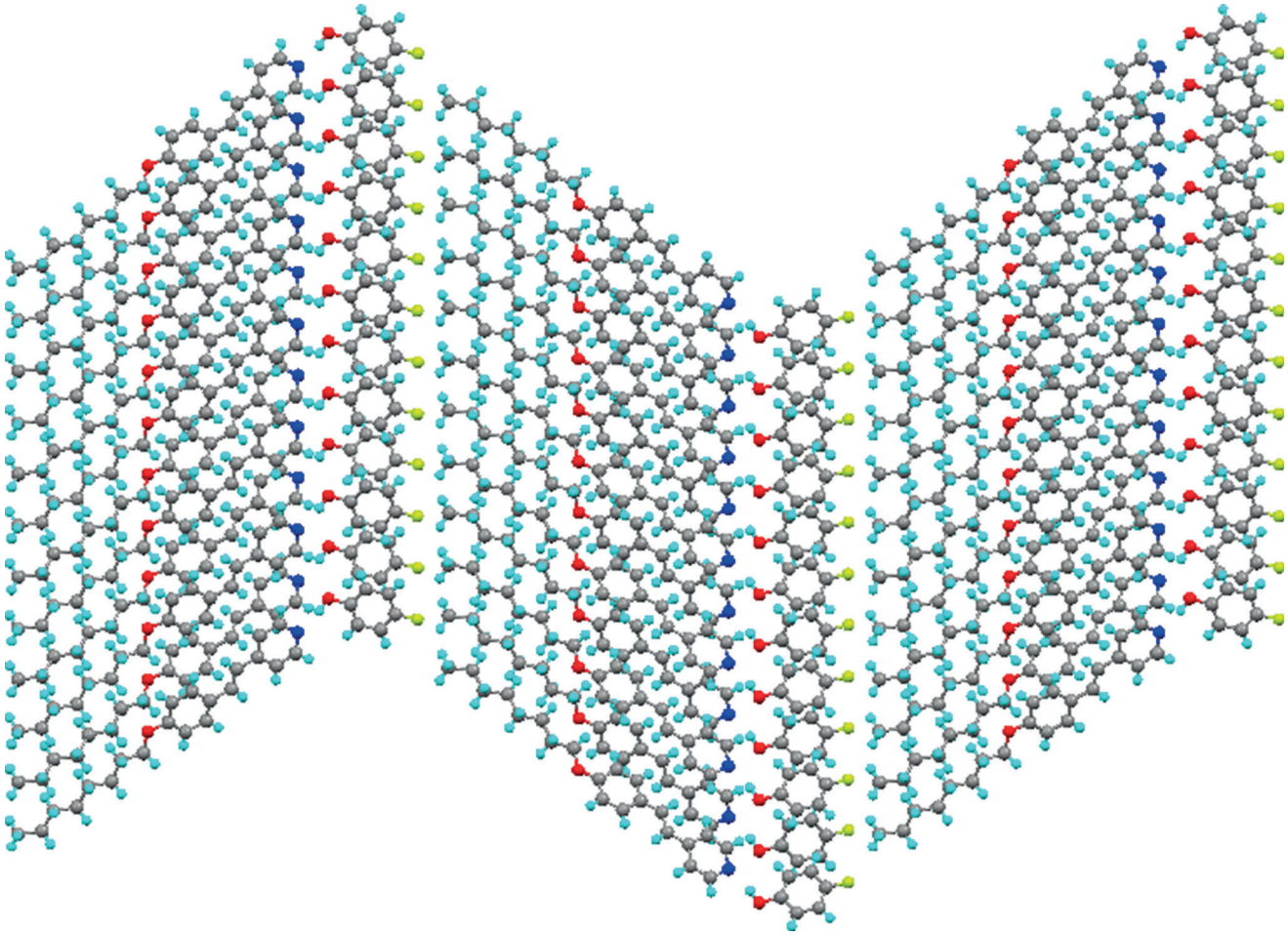

Figure 19. Ziz-zag packing of complex **2-4c** in the *bc* plane.

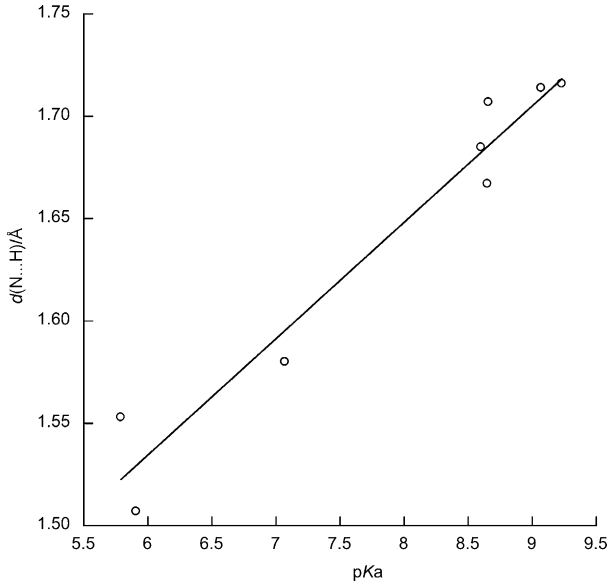

Figure 20. Plot of pK_a versus N···H hydrogen bond length; the correlation coefficient is 0.973.

Liquid-crystal properties: The liquid-crystal properties of the complexes were determined by polarised optical microscopy and differential scanning calorimetry (DSC), and the data are collected in Table 2 to Table 4, whereas examples of DSC traces are given in the Supporting Information. In general, the complexes melted quite cleanly, which is indicative of well-formed, single-component materials that are stable in the solid state and are stable up to the melting point of the complex. In some cases, however, the melting range was broad and here it was not always possible to ascertain the precise behaviour giving rise to the event. For example, it can be the case that at a given temperature, the two separate components of the complex represent a thermodynamically more stable state than the complex itself and so decomplexation can occur to give the components, which may or may not then recombine at some higher temperature reforming the complex.[6a] In cases where the origin of the broad melting is clear then it is described, but where the exact origin is not apparent then the wide melting range is simply reported as observed. However, where there is broad melting behaviour and liquid-crystal properties are observed, then it was found that the transition into the liquid-crystal phase was always sharp, indicative of a melt containing a 1:1 complex.

11 of the 16 complexes of 4-butoxy-4′-stilbazole were nematic and 4 showed enantiotropic mesomorphism. Under the microscope, the nematic phase was observed to be very homeotropic, but displacing the cover slip on the sample produced a four-brush schlieren texture as shown in Figure 21 a. The occurrence of the nematic phase observed in this series is as expected for simple polar mesogens with short terminal chains.

Figure 22 is a graphical representation of the thermal data observed by microscopy arranged in order of decreasing

Table 2. Thermal data for the butyloxystilbazole complexes.

Compound	Transition[a]	T [°C][b]	ΔH [kJ mol^{-1}][c]	ΔS [J mol^{-1} K^{-1}]
1-8	Cr–Cr_1	61.4	7.6	73
	Cr_1–N	88.5	26.3	22
	N–Iso	91.0	–	–
1-7	Cr–Cr_1	55.0–58.0	7.9	24
	Cr_1–N	82.0	10.1	28
	N–Iso	87.2	0.1	0.4
1-6a	Cr–Iso	89.1	39.2	109
	(N–Iso)	(88.1)	–	–
1-6b	Cr–Iso	89.7	35.8	99
	(N–Iso)	(87.0)	–	–
1-6c	Cr–Iso	106–109	30.6	80
	(N–Iso)	(97.5)	–	–
1-6d	Cr–Cr_1	–	0.3	0.9
	Cr_1–Iso	91.5	29.5	81
	(N–Iso)	(82.6)	(0.5)	–
1-6e	Cr–Cr_1	66.0	0.7	2
	Cr_1–Iso	76.5	31.2	90
	(N–Iso)	(73.5)	–	–
1-5a	Cr–Cr_1	48.0	10.1	31
	Cr_1–N	74.5	20.7	59
	N–Iso	80.9	0.5	1
1-5b	Cr–Cr_1	–	0.3	1
	Cr_1–Iso	87.0–93.0	28.0	77
1-5c	Cr–Cr_1	–	0.3	0.8
	Cr_1–Cr_2	–	0.5	1
	Cr_2–N	91.9	24.0	66
	N–Iso	95.9	0.7	2
1-5d	Cr–Iso	89.8	30.6	85
1-5e	Cr–Cr_1	63.5–72.5	4.2	12
	Cr_1–Iso	(broad)	35.0	101
	(N–Iso)	(69.7)	–	–
1-5f	Cr–Iso	82.0–84.5 (broad)	40.1	113
	(N–Iso)	(79.7)	(0.6)	–
1-4a	Cr–Cr_1	–	0.6	2
	Cr_1–Cr_2	–	2.1	6
	Cr_2–Iso	101 (very broad)	20.2	54
1-4b	Cr–Cr_1	–	0.1	0.5
	Cr_1–Iso	62.3	4.2	12
1-4c	Cr–Iso	101.0	37.7	101

[a] Observations and temperatures are from optical microscopy. [b] As far as possible, monotropic transition temperatures quoted are the true thermodynamic temperatures obtained by reheating to isotropic from the supercooled nematic phase and are indicated as heating transitions, for example, (N–Iso). [c] Occasionally enthalpies for clearing transitions could not be determined by DSC, but in most cases this was for monotropic transitions.

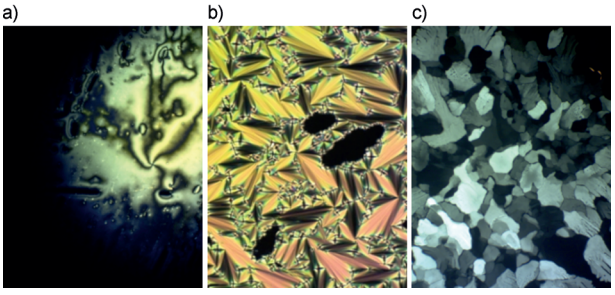

Figure 21. a) Schlieren nematic texture of complex **1-8** on cooling; b) the focal conic fan texture of the SmA phase c) the mosaic texture of the crystal smectic E phase of **2-4c**.

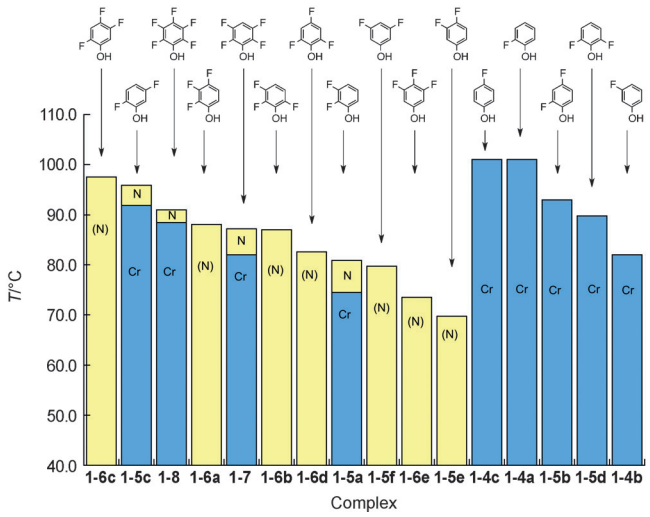

Figure 22. Graphical representation of the thermal behaviour of butyloxystilbazole complexes of the fluorophenols.

clearing point for the complexes that were mesomorphic (melting point is omitted for those showing monotropic phases) with those that are non-mesomorphic placed at the right-hand side. Thus, only complexes **1-5c**, **1-8**, **1-7** and **1-5a** showed enantiotropic phases, which is in reality a commentary on the stability of the crystal phase so that it is observed that these complexes have the least stable crystalline phases. The trifluorophenol complexes were all monotropic, and of these the 2,4,5-substituted fluorophenol complex, **1-6c**, had the highest clearing temperature at 97.5 °C. The difluorophenol complexes exhibited a mixture of enantiotropic, monotropic and non-mesomorphic behaviour with complex **1-5c** clearing at the highest temperature, exhibiting an enantiotropic nematic phase between 91.9 and 95.9 °C. The monosubstituted fluorophenol complexes were all non-liquid crystalline. Trends in liquid-crystal phase stability will be discussed below, but one immediate observation is that for all the complexes that were liquid crystalline, highest clearing points were found for those with a 2-fluoro substituent.

Thermal data for the complexes of octyloxystilbazole are collected in Table 3 and the data are plotted as a function of decreasing clearing point in Figure 23. Clearing points for complexes of **2** are, in general, slightly higher than those of stilbazole **1**, but there are two important differences, namely that crystal phases are destabilised by the increase in chain length as witnessed by the fact that all but one complex showed enantiotropic mesomorphism and that, as might have been anticipated, SmA phases (Figure 21b) are now seen in addition to the nematic. The order of decreasing clearing point does not follow the same progression as in Figure 22 for complexes of **1**, which will be discussed later. The only other significant difference is that for complex **2-4c**, a monotropic crystal smectic E phase is observed. This phase, characterised by its mosaic texture with feathered ends (Figure 21c), is also shown by the pure ligand,[15] but

Table 3. Thermal data for the 4-octyloxy-4′-stilbazole complexes.

Compound	Transition	T [°C]	ΔH [kJ mol^{-1}]	ΔS [J mol^{-1} K^{-1}]
2-8	Cr–N	87.5	40.2	112
	N–Iso	91.5	0.3	1
2-7	Cr–Cr_1	–	5.2	15
	Cr_1–Cr_2	–	3.7	11
	Cr_2–N	90.4	40.8	112
	N–Iso	90.6	–	–
2-6a	Cr–Cr_1	–	18.1	54
	Cr_1–SmA	65.1	19.8	59
	SmA–N	86.9	0.6	2
	N–Iso	92.7	1.2	3
2-6b	Cr–SmA	65.3	35.3	105
	SmA–N	86.7	0.5	1
	N–Iso	92.3	0.7	2
2-6c	Cr–Cr_1	–	12.9	38
	Cr–SmA	90.6	26.6	73
	SmA–N	95.6	0.8	2
	N–Iso	99.3	1.2	3
2-6d	Cr - SmA	60.1	36.3	109
	SmA - N	88.5	1.8	5
	N–Iso	89.7	1.7	5
2-6e	Cr–N	75.5	45.1	129
	N–Iso	81.1	0.7	2
2-5a	Cr–SmA	73.5	41.4	119
	SmA–N	78.9	0.2	0.7
	N–Iso	86.4	0.8	2.28
2-5b	Cr - Iso	94.7	14.2	39
2-5c	Cr–Cr_1	76.9	30.9	89
	Cr_1–SmA	92.0	10.5	29
	SmA–N	96.0	1.3	4
	N–Iso	99.3	1.0	3
2-5d	Cr–SmA	61.5	38.9	115
	SmA–Iso	91.0	5.0	14
2-5e	Cr–N	61.2	41.6	124
	N–Iso	76.7	0.7	2
2-5f	Cr–Iso	93.0	52.7	144
	(N–Iso)	(81.1)	(0.7)	(2)
2-4a	[*]	65.5	24.3	72
	Cr–Iso	95.2	13.8	37
2-4b	Cr–Cr_1	–	0.1	0.4
	Cr_1–Cr_2	–	1.9	6
	Cr_2–Iso	76.5	44.7	128
	(N–Iso)	(78.9)	–	–
	(SmA–N)	(64.2)	–	–
	(E–SmA)	(48.0)	–	–
2-4c	Cr–Iso	89.5	43.2	119

[a] Observations and temperatures are from optical microscopy. [b] As far as possible, monotropic transition temperatures quoted are the true thermodynamic temperatures obtained by reheating to isotropic from the supercooled nematic phase and are indicated as heating transitions, for example, (N–Iso). [c] Occasionally enthalpies for clearing transitions could not be determined by DSC, but in most cases this was for monotropic transitions. [*] Not observed by microscopy. Described in text.

the temperatures at which it is seen and also the behaviour observed mean that it is certainly part of the mesomorphic behaviour of the complex.

As in the previous series, the complexes with pentafluorophenol and 2,3,5,6-tetrafluorophenol showed an enantiotropic nematic phase, this time between 87.5–91.5 and 90.4–90.6 °C, respectively. On the other hand, the trifluorinated derivatives were all enantiotropic, as the longer alkyl chain length diminished crystal phase stability to lower the melt-

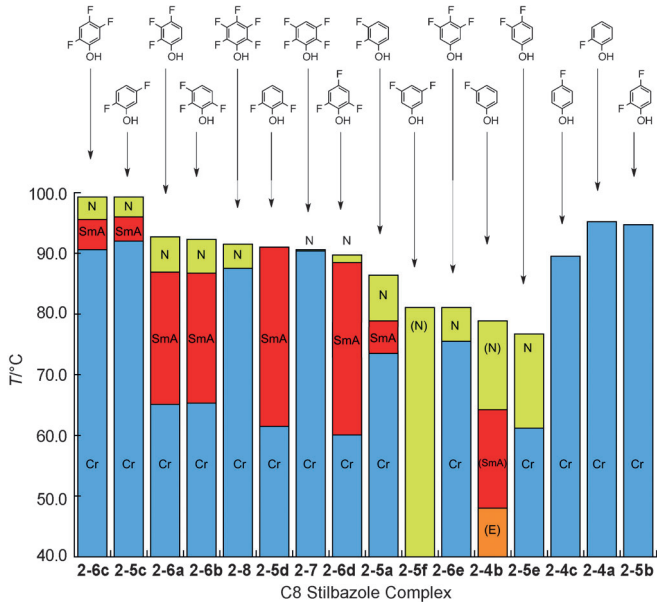

Figure 23. Graphical representation of the thermal behaviour of octyloxystilbazole complexes of the fluorophenols.

ing point. The difluorophenol derivatives were still a mixture of enantiotropic, monotropic and non-mesomorphic complexes whereas the mono-fluorinated derivatives remained non-mesomorphic with the exception of **2-4b**, which exhibited monotropic E, SmA and N phases.

Thermal data for complexes of dodecyloxystilbazole are collected in Table 4 and are plotted in Figure 24, once more in order of descending clearing point. Again as might be predicted on increasing the terminal chain length further, SmA phases were promoted strongly so that now only three complexes show a nematic phase. Indeed, the strong stabili-

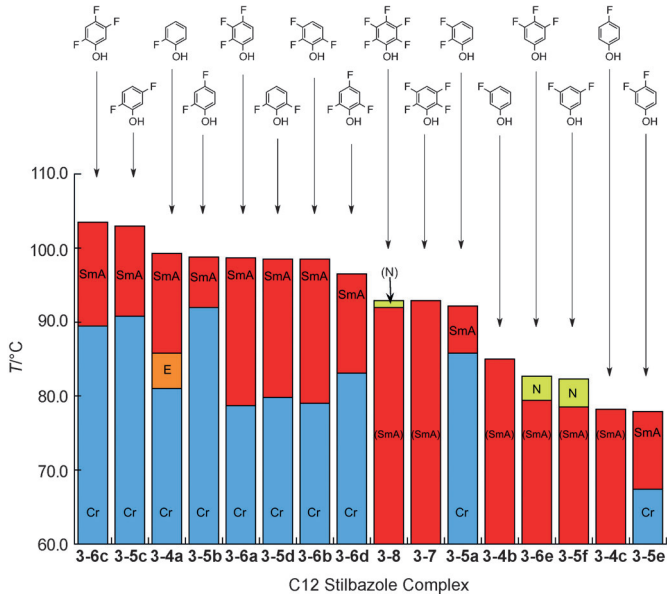

Figure 24. Graphical representation of the thermal behaviour of dodecyloxystilbazole complexes of the fluorophenols.

Table 4. Thermal data for the 4-dodecyloxy-4′-stilbazole complexes.

Compound	Transition	T [°C]	ΔH [kJ mol^{-1}]	ΔS [J mol^{-1} K^{-1}]
3-8	Cr–Iso	97.8 (broad)	50.9	138
	(N–Iso)	(92.9)	–	–
	(SmA–N)	(92.0)	–	–
3-7	Cr–Iso	95.5	48.1	131
	(SmA–Iso)	(92.9)	–	–
3-6a	Cr–SmA	78.7	53.9	153
	SmA–Iso	98.7	5.0	13
3-6b	Cr–SmA	79.0	55.5	158
	SmA–Iso	98.5	5.1	14
3-6c	Cr–Cr_1	–	1.2	4
	Cr_1–Cr_2	–	0.4	1
	[*]	87.0–89.5	31.3	87
	SmA–Iso	103.5	6.2	16
3-6d	Cr–Cr_1	–	0.5	1
	Cr_1–SmA	83.1	42.7	120
	SmA–Iso	96.5	5.2	14
3-6e	Cr–Iso	86.0	63.9	179
	(N–Iso)	(82.7)	–	–
	(SmA -N)	(79.4)	–	–
3-5a	Cr–Cr_1	–	0.2	0.6
	Cr_1–SmA	85.8	58.8	164
	SmA–Iso	92.2	5.5	15
3-5b	Cr–Cr_1	–	25.2	74
	Cr_1–Cr_2	–	27.9	80
	Cr_2–SmA	92.0	9.7	27
	SmA–Iso	98.8	7.3	20
	(E–SmA)	(93.2)	9.9	27
3-5c	Cr–SmA	90.8	49.5	137
	SmA–Iso	103.0	6.0	16
3-5d	Cr–SmA	79.8	55.4	157
	SmA–Iso	98.5	7.0	19
3-5e	Cr–SmA	65.0–67.4	55.1	162
	SmA–Iso	77.9	3.3	10
3-5f	Cr–Iso	100.0	75.0	202
	(N–Iso)	(82.3)	–	–
	(SmA–N)	(78.5)	–	–
3-4a	Cr–E	81.0	48.7	137
	E–SmA	94.5	9.3	25
	SmA–Iso	99.3	9.0	24
3-4b	Cr–Iso	88.0	70.1	194
	(SmA–Iso)	(85.0)	–	–
3-4c	Cr–Iso	94.3	64.5	176
	(SmA–Iso)	(78.2)	–	–

[a] Observations and temperatures are from optical microscopy. [b] As far as possible, monotropic transition temperatures quoted are the true thermodynamic temperatures obtained by reheating to isotropic from the supercooled nematic phase and are indicated as heating transitions, for example, (N–Iso). [c] Occasionally enthalpies for clearing transitions could not be determined by DSC, but in most cases this was for monotropic transitions. [*] Not observed by microscopy. Described in text.

sation of the SmA phase combined with some destabilisation of the crystal phase means that none of the complexes derived from stilbazole **3** was monotropic. Once more, a crystal smectic E phase was observed, this time for complexes **3-5b** and **3-4a** and its monotropic nature in the former does not allow it easily to be displayed on the graph. In both complexes, the fact that the E phase melts into the SmA phase above the temperature at which the crystal E phase of the pure ligand forms an isotropic liquid, once more demonstrates that the phase is a property of the individual complexes.

The behaviour of complex **3-6c** warrants further comments, so that in the temperature range 87.0 to 89.5 °C, it was observed to melt in two stages before forming a SmA phase. Optical microscopy supported the view that at 87 °C, the hydrogen bond of the solid complex broke to give the liquid phenol plus the solid stilbazole and then, as the temperature was raised, the stilbazole itself melted. With both components in the fluid phase, the hydrogen bond then reformed and the complex shows a SmA phase. This is explained as up to 87 °C, the crystalline phase of the hydrogen-bonded complex was the stable state. Above this temperature, it was preferable thermodynamically for the two components to exist as the solid form of the stilbazole and the free phenol until the stilbazole melted, at which point the two components hydrogen bonded once more, revealing the mesophase.

What is interesting here is that Figure 24 shows a very different order of complexes along the *x* axis, which will form part of the discussion below.

Discussion

Generally, the hydrogen-bonded complexes prepared were observed to clear at increasing temperatures with increasing alkoxy chain length. The 4-butoxy-4′-stilbazole complexes were mostly nematogenic, the 4-octyloxy-4′-stilbazole complexes exhibited both the nematic and smectic A phase, whereas the majority of the 4-dodecyloxy-4′-stilbazole complexes displayed only the smectic A phase. This evolution in thermal behaviour as a function of alkoxy chain length for the complexes of **5c** is shown in Figure 25.

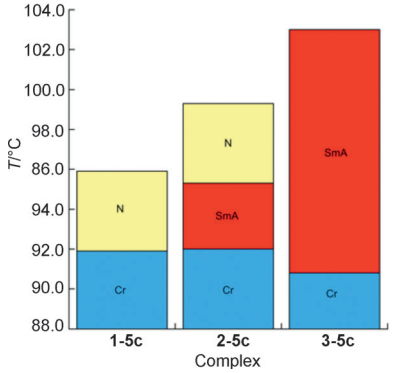

Figure 25. Evolution of the thermal behaviour.

However, more significant is to try to understand how the clearing point varies with the nature of the fluorophenol. Thus, Figures 22 to 24 show clearing points in descending order and, close examination of the data reveal a very good degree of conformity between the three and changes in order are in most cases minimal. For example, clearing points decrease as follows (complexes that appear in one line but not the one above are in italics):

C4 stilbazole: **1-6c** > **1-5c** > **1-8** > **1-6a** > **1-7** > **1-6b** > **1-6d** > **1-5a**

C8 stilbazole: **2-6c** > **2-5c** > **2-6a** > **2-6b** > **2-8** > ***2-5d*** > **2-7** > **2-6d** > **2-5a**

C12 stilbazole: **3-6c** > **3-5c** > ***3-4a*** > ***3-5b*** > **3-6a** > **3-5d** > **3-6b** > **3-6d** > **3-8** > **3-7** > **3-5a**

Thus, although in series **2** there is some change in the order with respect to **2-8** and **2-7**, inspection of the graph shows that all complexes from **2-6a** to **2-6d** have very similar clearing points and so the change is not regarded as significant. Similar arguments hold for **3-4a** to **3-6b**, although in series **3** the clearing point of complexes **3-8** and **3-7** are appreciably lower.

However, what is perhaps more revealing is to plot the data as a function of decreasing clearing point but also according to the number of fluorine atoms attached to the fluorophenol. This is shown in Figure 26 for complexes of

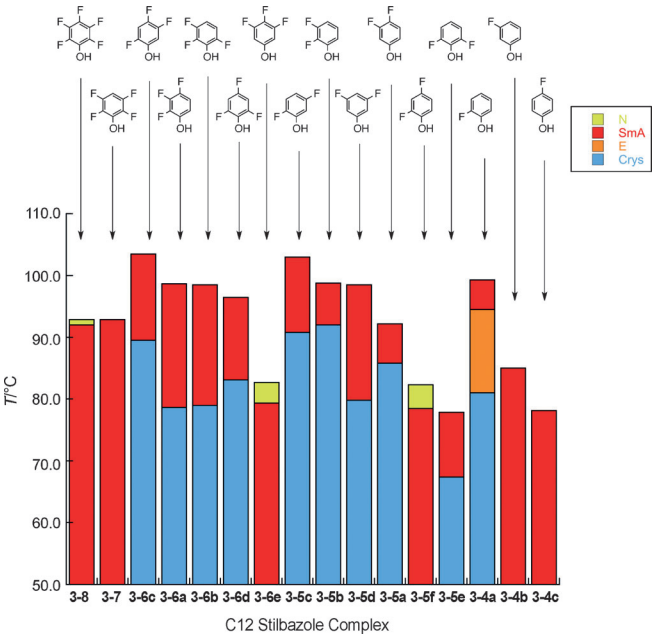

Figure 26. Clearing point plotted in descending order according to the number of fluorine atoms on the fluorophenol for complexes of series **3**.

series **3** and as Figures S7 and S8 (in the Supporting Information) for complexes of series **1** and **2**, respectively. What is remarkable is that in each series, the order is absolutely identical (obviously only complexes with mesophases will fit such an analysis).

So how can this behaviour be understood? Figure 27 shows the different complexes organised by number of fluorine atoms and clearing point and allows a more insightful structural comparison. What is clear is that for phenols **5** and **6**, the highest clearing points are always found where there is a fluorine atom in the 2-position and, as indicated in the figure, this is interpreted as arising from the formation of an additional, intramolecular hydrogen bond between

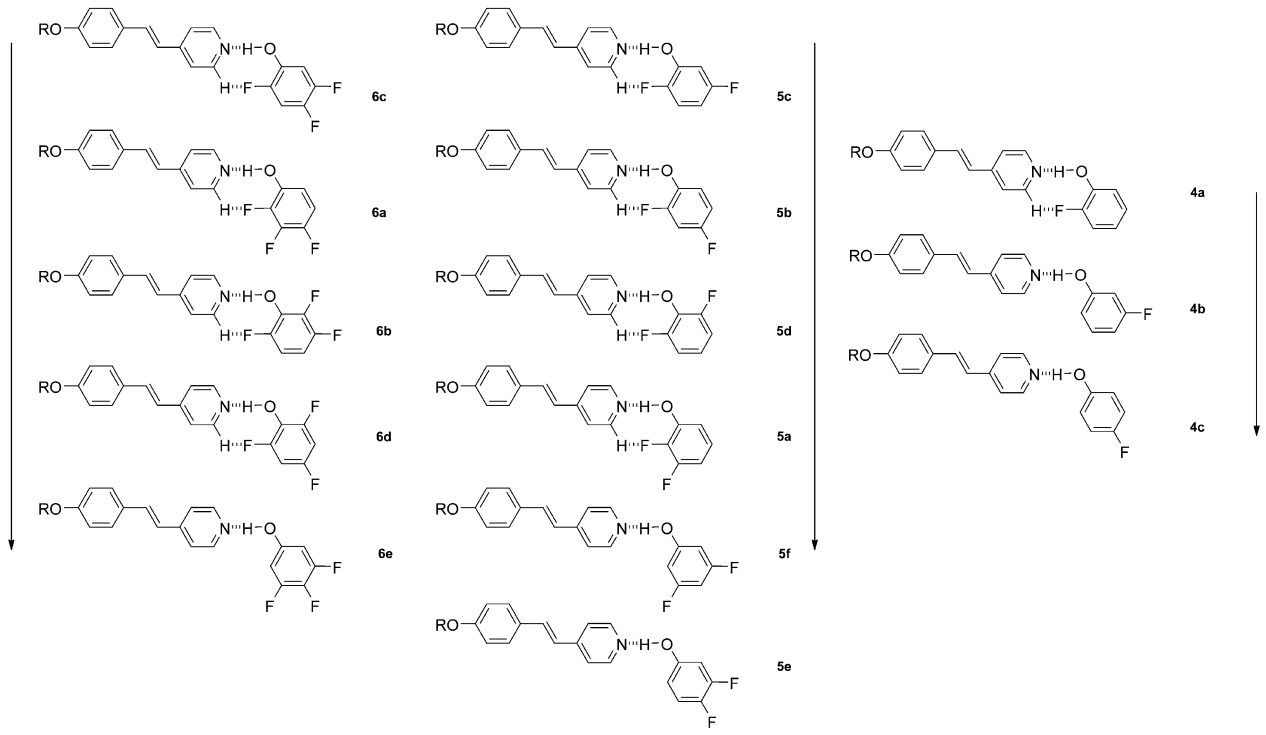

Figure 27. Hydrogen-bonded complexes arranged in order of decreasing clearing point and by number of fluorine atoms, with phenols **7** and **8** omitted.

this 2-fluorine and the *ortho*-hydrogen of the pyridine ring in the stilbazole. That such a motif is a reasonable proposition is supported by its observation in the crystal structures of complexes **2-8** and **2-7** in which the intramolecular F···H distance is 2.234 and 2.36 Å, respectively. The presence of such an interaction would give a more rigid structure to the mesogen when compared to the much more flexible arrangement that would be expected through a single point of contact, which is consistent with the higher clearing points. Beyond this, the mesophases are clearly most stabilised when the phenol contains a 3-fluorophenol or 4-fluorophenol motif, both of which provide a terminal dipole that will enhance the dielectric anisotropy.[1]

Finally, it is appropriate to determine if there is any correlation between the pK_a of the phenol and the clearing point, as from time to time in the literature it has been speculated that the clearing of a liquid crystal phase has been driven by the rupture of the hydrogen bond. Figure 28 shows the calculated pK_a values for the different fluorophenols plotted against the clearing point for complexes of series **2** and **3**; the analogous plot for series **1** complexes is found as Figure S8 (in the Supporting Information). Analysis of the data reveals that they can be considered in two groups. The first of these consists of phenols with a 2-fluoro substituent which, as noted above, tend to give complexes with higher clearing points, whereas the second group consists of complexes in which the phenol does not have a 2-fluoro substituent and where clearing points are lower for the reasons explained earlier. For clarity, these two regions are separated in the figures by a dotted line. However, within or between these groups there is no dependence of the clearing point on pK_a.[2] Thus, in common with our earlier finding and assertions,[5a,b] we see no evidence whatsoever that clearing of these complexes is driven by anything other than the natural clearing behaviour of the hydrogen-bonded complex.

Conclusion

This exhaustive and systematic study of the structure and mesomorphism of fluorophenol complexes of alkoxystilbazoles has provided a good deal of information about the behaviour of these new, hydrogen-bonded species. By virtue of the fact that all but one of the complexes of series **2** that were crystallised did so in the $P\bar{1}$ space group, meaningful comparisons could be made. Central to the results of this study was the proposition that in many cases, what appeared to be real, intermolecular interactions were unlikely to be of any real significance in determining crystal packing and, consequently, care is suggested in interpreting such interactions in future studies.

[1] Although it is, in general, much less reliable to seek trends in melting points, we did look at them for complexes **2-5a**, **2-5d**, **2-5f**, **2-4a** and **2-4b** (all of which crystallise in $P\bar{1}$) and found no correlation with the planarity of the complex induced by the presence of a fluorine in the 2-position.

[2] The data for series **1** (Figure S8 in the Supporting Information) show a less clear separation between the two regions, but the form of the plot is otherwise identical.

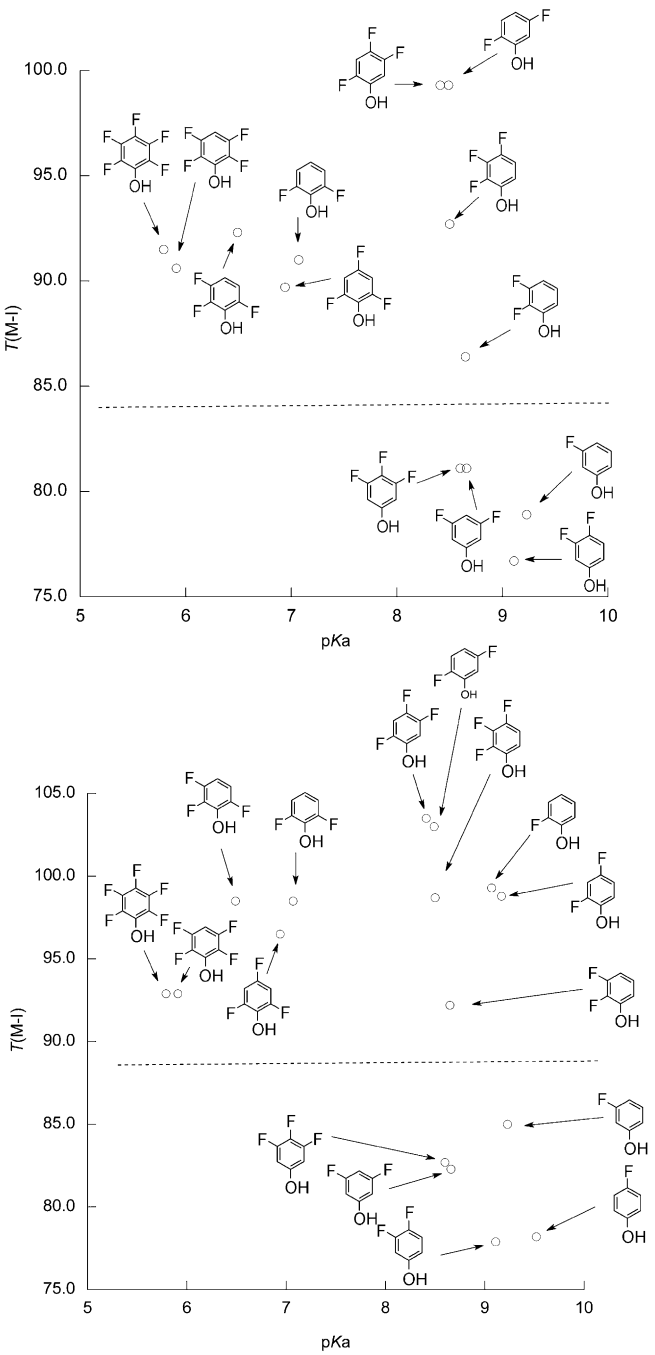

Figure 28. Plot of clearing point as a function of pK_a for complexes of (left) octyloxystilbazole (**2**) and (right) dodecyloxystilbazole (**3**).

In terms of liquid-crystal properties, in general terms the overall pattern of mesomorphism in relation to stilbazole chain length was as might have been expected for such simple, dipolar mesogens. Thus, nematic phases were favoured at short chain lengths, whereas the SmA phase became stabilised when the terminal alkoxy chain was much longer. More interesting was the dependence of mesophase stability (N or SmA) on the fluorophenol. With small exceptions for complexes of pentafluorophenol (**8**) and 2,3,5,6-tetrafluorophenol (**7**), a very similar dependence of clearing point on phenol was observed in all series and, more strikingly, exactly the same dependence of clearing point on fluorine substitution pattern for a given number of fluorine atoms was found for each of the three stilbazole chain lengths studied. In particular, it was noted that mesophases were most stable where the phenol had a 2-fluorine substituent, which was interpreted in terms of the added stability provided by the formation of an intramolecular six-membered ring involving the phenol and the stilbazole, possibly due to this pattern of substitution.

Finally, it was noted that there was no dependence of the clearing point on the pK_a of the phenol and, by extension, the strength of the N···H hydrogen bond. This offers strong support to previous assertions from this group[5a,b] that clearing in hydrogen-bonded mesogens is of the hydrogen-bonded complex and is not driven by hydrogen-bond rupture.

Experimental Section

All the fluorophenols were used as received from Fluorochem and alkoxystilbazoles were prepared as described previously.[15] ^{1}H NMR spectra were recorded at 270 MHz using a JEOL ECX270 instrument, whereas optical microscopy employed an Olympus BX50 Optical Microscope equipped with a Link-Am HFS91 hot stage, TMS92 controller and LNP2 cooling unit. DSC data were collected using a Mettler Toledo DSC 822, equipped with a TSO801R0 sample robot and calibrated using indium; samples were run at heating and cooling rates of 10 °C min^{-1}. Elemental analysis was carried out on an Exeter Analytical Inc CE 440 Elemental Analyser and a Sartorius SE2 analytical balance at the University of York.

Diffraction data were collected at 110 K on a Bruker Smart Apex diffractometer with $Mo_{K\alpha}$ radiation ($\lambda = 0.71073$ Å) using a SMART CCD camera. Diffractometer control, data collection and initial unit cell determination was performed using "SMART".[16] The crystal was cooled with an Oxford Crysostream. Frame integration and unit-cell refinement was carried out with "SAINT+".[17]Absorption corrections were applied by SADABS.[18] Structures were solved by "direct methods" using SHELXS-97 (Sheldrick, 1997)[19] and refined by full-matrix least squares using SHELXL-97 (Sheldrick, 1997).[20] All non-hydrogen atoms were refined anisotropically. O–H hydrogen atoms were located by difference map after all other atoms had been located and refined. All other hydrogen atoms were placed using a "riding model" and included in the refinement at calculated positions. Three of the structures exhibited disorder, which was modelled as follows:

2-8: Both of the aromatic rings and the double bond of the stilbene exhibited disorder and were modelled in two positions, the relative occupancy of which refined to 0.77:0.23. For the minor component, the aromatic rings were constrained to be regular hexagons with a bond length of 1.39 Å. The anisotropic displacement parameters of corresponding pairs of disordered atoms for example, C7a and C7b were constrained to be equal.

2-5a: The difluorophenyl group was disordered by rotation about the C_{ipso}–C_{para} axis and was modelled in two positions with a refined relative occupancy of 84:16.

2-4b: The position of the fluorine was disordered over the two possible *meta* positions. The relative occupancy of the positions was refined to 3:1.

Acknowledgements

J.P.-W.W. thanks the University of York, Department of Chemistry's Wild Fund for financial assistance.

[1] D. W. Bruce in: *Supramolecular Chemistry: From Molecules to Nanomaterials* (Eds.: J. W. Steed and P. A. Gale), Wiley, Chichester, **2012**, pp. 3493–3514.
[2] For a recent review, see: A. C. Legon, *Phys. Chem. Chem. Phys.* **2010**, *12*, 7736.
[3] a) P. Metrangolo, H. Neukirch, T. Pilati, G. Resnati, *Acc. Chem. Res.* **2005**, *38*, 386; b) P. Metrangolo, G. Resnati, *Science* **2008**, *321*, 918.
[4] a) T. Kato, J. M. J. Fréchet, *J. Am. Chem. Soc.* **1989**, *111*, 8533; b) T. Kato, J. M. J. Fréchet, *Macromolecules* **1989**, *22*, 3818; c) U. Kumar, T. Kato, J. M. J. Fréchet, *J. Am. Chem. Soc.* **1992**, *114*, 6630; d) T. Kato, H. Kihara, T. Uryu, A. Fuijishima, J. M. J. Fréchet, *Macromolecules* **1992**, *25*, 6836; e) T. Kato, H. Kihara, U. Kumar, T. Uryu, J. M. J. Fréchet, *Angew. Chem.* **1994**, *106*, 1728; *Angew. Chem. Int. Ed. Eng.* **1994**, *33*, 1644; f) T. Kato, P. G. Wilson, A. Fuijishima, J. M. J. Fréchet, *Chem. Lett.* **1990**, 2003; g) T. Kato, J. M. J. Fréchet, P. G. Wilson, T. Saito, T. Uryu, A. Fuijishima, C. Sin, F. Kaneuch, *Chem. Mater.* **1993**, *5*, 1094; h) T. Kato, A. Fuijishima, J. M. J. Fréchet, *Chem. Lett.* **1990**, 912; i) M. Fukumasa, T. Kato, T. Uryu, J. M. J. Fréchet, *Chem. Lett.* **1993**, 65; j) T. Kato, H. Kihara, T. Uryu, S. Ujiie, K. Iimura, J. M. J. Fréchet, U. Kumar, *Ferroelectrics* **1994**, *148*, 1303.
[5] a) D. J. Price, K. Willis, T. Richardson, G. Ungar, D. W. Bruce, *J. Mater. Chem.* **1997**, *7*, 883; b) D. J. Price, T. Richardson, D. W. Bruce, *J. Chem. Soc. Chem. Commun.* **1995**, 1911; c) D. W. Bruce, D. J. Price, *Adv. Mater. Opt. Electron.* **1994**, *4*, 273.
[6] a) D. J. Price, H. Adams, D. W. Bruce, *Mol. Cryst., Liq. Cryst.* **1996**, *289*, 127; b) K. Willis, J. E. Luckhurst, D. J. Price, J. M. J. Fréchet, T. Kato, G. Ungar, D. W. Bruce, *Liq. Cryst.* **1996**, *21*, 585; c) B. Friot, D. Boyd, K. Willis, B. Donnio, G. Ungar, D. W. Bruce, *Liq. Cryst.* **2000**, *27*, 605.
[7] For example, see: a) M. Suárez, J. M. Lehn, S. C. Zimmerman, A. Skoulios, B. Heinrich, *J. Am. Chem. Soc.* **1998**, *120*, 9526; b) D. Goldmann, D. Janietz, C. Schmidt, J. H. Wendorff, *J. Mater. Chem.* **2004**, *14*, 1521; c) S. Coco, C. Cordovilla, C. Domínguez, B. Donnio, P. Espinet, D. Guillon, *Chem. Mater.* **2009**, *21*, 3282.
[8] H. L. Nguyen, P. N. Horton, M. B. Hursthouse, A. C. Legon, D. W. Bruce, *J. Am. Chem. Soc.* **2004**, *126*, 16.
[9] a) D. W. Bruce, P. Metrangolo, F. Meyer, T. Pilati, C. Präsang, G. Resnati, G. Terraneo, S. G. Wainwright, A. C. Whitwood, *Chem. Eur. J.* **2010**, *16*, 9511; b) C. Präsang, H. L. Nguyen, P. N. Horton, A. C. Whitwood, D. W. Bruce, *Chem. Commun.* **2008**, 6164; c) C. Präsang, A. C. Whitwood, D. W. Bruce, *Chem. Commun.* **2008**, 2137; d) D. W. Bruce, P. Metrangolo, F. Meyer, C. Präsang, G. Resnati, A. C. Whitwood, *New J. Chem.* **2008**, *32*, 477; e) P. Metrangolo, C. Präsang, G. Resnati, R. Liantonio, A. C. Whitwood, D. W. Bruce, *Chem. Commun.* **2006**, 3290.
[10] a) J. Xu, X. Liu, J. Kok-Peng Ng, T. Lin, C. He, *J. Mater. Chem.* **2006**, *16*, 3540; b) J. Xu, X. Liu, T. Lin, J. Huang, C. He, *Macromolecules* **2005**, *38*, 3554.
[11] C. Präsang, A. C. Whitwood, D. W. Bruce, *Cryst. Growth Des.* **2009**, *9*, 5319.
[12] J. Han, F. M. Tao, *J. Phys. Chem. A* **2006**, *110*, 257.
[13] a) M. J. G. Lesley, A. Woodward, N. J. Taylor, T. B. Marder, I. Cazenobe, I. Ledoux, J. Zyss, A. Thornton, D. W. Bruce, A. K. Kakkar, *Chem. Mater.* **1998**, *10*, 1355; b) D. W. Bruce, R. G. Denning, M. G. Grayson, R. Le Lagadec, K. K. Lai, B. T. Pickup, A. Thornton, *Adv. Mater. Opt. Electron.* **1994**, *4*, 293; c) D. W. Bruce, A. Thornton, *Mol. Cryst., Liq. Cryst.* **1993**, *231*, 253.
[14] Overlaying was achieved using the application QtMG available free from: http://www.ccp4.ac.uk/MG.
[15] D. W. Bruce, D. A. Dunmur, E. Lalinde, P. M. Maitlis, P. Styring, *Liq. Cryst.* **1988**, *3*, 385.
[16] "SMART": control software Bruker SMART Apex X-ray Diffractometer. v5.625, Bruker-AXS GMBH, Karlsruhe, Germany.
[17] "SAINT+": integration software for Bruker SMART detectors. v6.45, Bruker-AXS GMBH, Karlsruhe, Germany.
[18] "SADABS": program for absorption correction. v2.10. G. M. Sheldrick, Bruker AXS Inc., Madison, Wisconsin, USA, **2007**.
[19] SHELXS-97: program for structure solution. G. M. Sheldrick, University of Göttingen, Göttingen, Germany, **1997**.
[20] SHELXL-97: program for the Refinement of Crystal Structures. G. M. Sheldrick, University of Göttingen, Göttingen, Germany, **1997**.

Received: August 2, 2012
Published online: October 19, 2012

